

Calculated band structure of zinc-blende-type SnGe

T. Brudevoll, D. S. Citrin,* N. E. Christensen,† and M. Cardona

Max-Planck-Institut für Festkörperforschung, Heisenbergstraße 1, D-70569 Stuttgart, Federal Republic of Germany

(Received 8 July 1993)

The band structure of SnGe in the zinc-blende structure is calculated using the scalar-relativistic linear-muffin-tin-orbital method in conjunction with the density-functional scheme. The local-density approximation is empirically corrected by means of an external potential. Special emphasis is placed on the effects of inversion asymmetry, such as ionicity and spin splittings. An equilibrium volume is found at a lattice constant of $a_0 = 6.0630 \text{ \AA}$, which is very close to the average of the lattice constants of Ge and α -Sn. At the corresponding volume, the calculated direct gap is $+0.085 \text{ eV}$. For a slightly larger lattice constant, corresponding to the average volumes of the two constituents, SnGe should have a “negative” gap of nearly the same magnitude, and thus have an inverted band structure similar to α -Sn. The polarity of the Ge-Sn bond is calculated to be $\alpha_p = 0.2$. The transverse effective charge is $e_T^* = 0.47$, Sn being positive (“cation”).

I. INTRODUCTION

The band structures of $\text{Sn}_x\text{Ge}_{1-x}$ alloys are of interest because of the possibility of varying the band gaps by varying the Sn concentration. Thus a transition from an indirect to a direct gap is expected when the concentration x of Sn is varied between 0 and 1.¹⁻⁶ SnGe in the zinc-blende structure is the second noncentrosymmetric group-IV compound for which the spin splittings have been investigated. Earlier⁷ calculations were presented for another noncentrosymmetric IV-IV compound, namely, GeSi. Here we compare the calculated spin splittings and ionicities of SnGe and GeSi.

The SnGe compound can be regarded as a prototype for all noncentrosymmetric Sn_n/Ge_m (n, m odd) superlattices; however, its cubic structure is unaffected by the internal strain built into Sn_n/Ge_m superlattices as a result of the large lattice mismatch. This means that the band structure is not complicated by the effects of uniaxial strains at the different layers under various conditions of pseudomorphic growth, and that relativistic spin splittings can be easily interpreted. Thus, a word of caution is in order when comparing our results with other calculations or with experiments. Alloy films of SnGe with $x=0.5$ should be comparable to our calculations, but these films have thus far been grown² on substrates with other lattice constants a_0 than that obtained from our total-energy calculation ($a_0 = 6.0630 \text{ \AA}$). As a result, the films will usually have a noncubic unit cell (tetragonally strained), as well as a different unit-cell volume. The gap E_0 is very sensitive to changes in unit-cell volume, just as it is sensitive to a change in alloy composition. On the one hand this indicates the possibility of large tunability of the optical properties for applications. On the other, one expects that the optical properties will be extremely sensitive to inhomogeneities in the samples. In this paper we have restricted ourselves to the ordered alloy $x = 0.5$ and to cubic unit cells at different volumes.

Bulk α -Sn (grey tin) is unstable at temperatures above 13.2°C ,⁸ where a transition to β -Sn (white tin) takes place, and so bulk α -Sn is not suited to many appli-

cations. By epitaxial growth of thin SnGe layers²⁻⁶ or Sn_m/Ge_n superlattices⁹⁻¹² the phase transition can be inhibited and the zinc-blende structure can exist at higher temperatures. The band structures of the SnGe alloys have been studied with a tight-binding model in the virtual-crystal approximation.¹ Because of the underlying assumption of identical average atoms in the unit cell, i.e., the assumption of a diamond lattice, a virtual-crystal approximation applied to a zinc-blende semiconductor cannot give the spin splittings related to the absence of inversion symmetry. To date, no self-consistent calculation of the SnGe compound has appeared in the literature.

In this paper we present *ab initio* total-energy calculations performed with the full-potential linear-muffin-tin-orbital (LMTO) method,^{13,14} as well as band-structure calculations within the atomic-sphere approximation (ASA). The total-energy calculations are used in Sec. II to predict the equilibrium unit-cell volume for the SnGe compound. Section III is devoted to the evaluation of effective masses and matrix elements of the momentum \mathbf{p} , and in Sec. IV the spin-orbit (SO) parameter Δ^- (for coupling between the Γ_{15} conduction and valence states) is calculated both with the LMTO method and with a simple tight-binding expression. The cubic and linear terms of the inversion-asymmetry spin splittings calculated along different lines in \mathbf{k} space are presented in Sec. V, together with estimates obtained with the $\mathbf{k}\cdot\mathbf{p}$ method. In Sec. VI we report calculations of the ionicity and transverse effective charge in SnGe. Finally, Sec. VII contains a summary of the results.

II. LMTO TOTAL-ENERGY AND BAND-STRUCTURE CALCULATIONS

The calculations presented here are closely related to those for GeSi in Ref. 7, but with the gap-correcting procedure modified as described for α -Sn in Ref. 15. Thus the values presented for the p - s (valence-band top to the first s -like conduction band) and p - p (valence-band top to the first p -like conduction band) gaps at $\mathbf{k} = \mathbf{0}$ are

to be regarded as the experimentally obtained values. In Ref. 7 and earlier LMTO calculations,¹⁸ the p - p gaps obtained were too small due to the well known inadequacies of the local-density approximation (LDA) to provide a good description of the excited states. Because of this we have also recalculated energy gaps, matrix elements, and masses for Ge; the most important ones appear in this paper. We treat the $3d$ levels of Ge as “frozen” corelike states (except in the full-potential LMTO total-energy calculations), whereas the Sn $4d$ levels are treated as fully relaxed band states. The splittings that we want to examine for the SnGe compound are due to inversion asymmetry and the SO interaction.

In order to obtain a consistent definition of the sign of the SO parameter Δ^- and the matrix elements P , P' , Q , and P''' , which are defined as¹⁹

$$\begin{aligned} P &= i\langle\Gamma_{15,x}^v|p_x|\Gamma_1\rangle, & P' &= i\langle\Gamma_{15,x}^c|p_x|\Gamma_1\rangle, \\ Q &= i\langle\Gamma_{15,x}^v|p_y|\Gamma_{15,z}^c\rangle, & P''' &= i\langle\Gamma_{15,x}^c|p_x|\Gamma_1'\rangle, \end{aligned} \quad (1)$$

it is necessary to specify the positions chosen for the two constituent atoms, and also the phase of the wave functions.^{7,18} Because of time-reversal symmetry we can conveniently choose them to be real, as depicted in Fig. 1. The Ge atom has been chosen to lie at the origin, while Sn is located at $a_0(\frac{1}{4}, \frac{1}{4}, \frac{1}{4})$ where a_0 is the lattice constant. This convention is consistent with the one used earlier,^{7,18} provided we call the Ge atom the “anion.” This choice results in a positive sign for P and Q , which can easily be verified from Fig. 1 by replacing p_x by $-id/dx$. (We use atomic units such that $\hbar = m_e = e = 1$, i.e., the hartree is the unit of energy, unless otherwise stated.)

As is well known, the energy gaps across the Fermi level calculated within the LDA are smaller than the

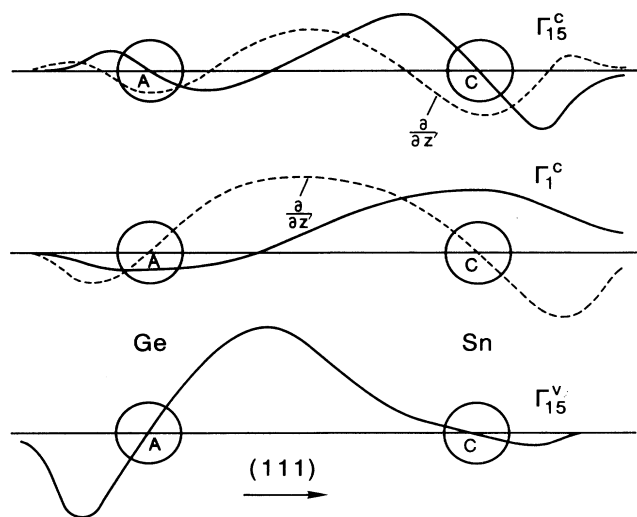


FIG. 1. Schematic diagram demonstrating the phase convention of the Γ_{15}^c , Γ_{15}^v , and Γ_1 wave functions. The Ge atom is taken to lie at the origin and corresponds to the anion (A). The cation (Sn) is labeled C. In the figure, the z' direction corresponds to (111).

experimentally measured values. This is compensated by adding external potentials²⁰ which are included self-consistently in the iteration procedure in the density-functional formalism. The extra potentials are chosen such that the important energy gaps in bulk α -Sn and Ge reproduce well the experimentally known values. These external potentials are then transferred, without modification, to the self-consistent calculations for the SnGe compound. This assumed transferability has been empirically justified by several examples.^{15,21,22} Table I shows the parameters used to correct the LDA gaps. In transferring these parameters to the calculations for the SnGe compound, we take the external potentials localized in the empty spheres of the two materials to be the same.¹⁵ In the empty spheres located at interstitial positions in the SnGe lattice the norm of the external correcting potential (defined as the potential integrated over the volume of the sphere) is to be regarded as a parameter common to a certain class of materials (such as semiconductors), whereas the correction potentials inside the occupied spheres are characteristic of the individual atoms. Although the procedure of lumping self-energy effects into a potential is not rigorous, we can still obtain significant improvements in the excitation energies by such an approach.^{15,20} Both local and dynamical effects are important for the explanation of the observed gaps.²³ We can only do justice to these effects in an average way here. The LDA potential is explicitly corrected as described in Ref. 15. Details of how the external potential is parametrized¹⁶ are given in Table I. Since we have used the ASA formulation in our band-structure calculations, the external potential must have spherical symmetry inside the spheres. Thus we are led to consider two types of potential, V_1 and V_2 , centered at occupied and empty spheres, respectively. Note that the mechanism bringing about the shift between valence and conduction states is the same as that responsible for the shift in the GW approximation; in a similar but more sophisticated way than our correction potential, the self-energy term exploits the difference in spatial localization of conduction and valence states and thereby leads to large shifts between these bands. (See, e.g., Ref. 23, in particular, the discussion of the Coulomb-hole term.)

In its present form, the correction in the unoccupied spheres is only appreciable within the outer $\sim 20\%$ of the sphere radius, and in occupied spheres it is concentrated near the sphere center. We know²³ that the LDA wave

TABLE I. External correction potential parameters V_o , V_e (hartree) and R_o , R_2 (bohr) [at the equilibrium sphere radius of 2.821 bohr (lattice constant $a_0 = 6.0630$ Å)].

	Atomic site ^a		Empty sphere ^b	
	V_o	R_o	V_e	R_2
Sn	142	0.015	0.0613	2.52
Ge	185	0.015	0.0613	2.52

^a $V_1(r) = V_o(R_o/r) \exp[-(r/R_o)^2]$.

^b $V_2(r) = V_e(r/R_2)^{10}$.

functions are already very close to those obtained using the *GW* approximation, and our correction procedure does not alter this fact. The virtue of the method used here is simplicity, an advantage which is very convenient when considering larger systems such as Sn_n/Ge_m superlattices.¹⁷ Our total-energy calculations were done within the LDA, i.e., without the adjusting potentials. It is of little relevance to calculate the ground state properties with these potentials included. We have, however, done that in a number of cases, and in general the correcting potentials increase the electronic pressure at a given volume. This produces an increase of 2–4% of the calculated equilibrium volume. The LDA causes an “overbinding,” the volumes being too small by a few percent. Thus, the correcting potentials tend to compensate for this. In view of the nature of our correction we consider this to be “accidental,” and of little physical significance. But for the calculation of optical properties²¹ it is of importance to note that the occupied states are only slightly shifted by the external potentials.

To evaluate the equilibrium volume of the SnGe compound we also performed full-potential^{14,24} LMTO total-energy calculations. The results are depicted in Fig. 2. A negative deviation of $\sim 1.1\%$ from the experimental equilibrium volumes of α -Sn and Ge was observed (cf. Table II). For the SnGe compound we therefore added the same deviation to the volume predicted by total-energy calculations and thus arrived at a lattice constant $a_0 = 6.063$ Å, which is close to the average of the Ge and α -Sn lattice constants. The calculations represented in Fig. 2 predicts that the energy change accompanying a decomposition of SnGe into bulk Sn and Ge (at their equilibrium volumes) is positive. A confirmation of this surprising result, though, requires improved accuracy of the total-energy calculations. (The decomposition enthalpy of GeSi is ≈ -2 mRy/f.u., i.e., GeSi is not stable.)

We have also calculated the band structure at other unit-cell volumes. The most interesting result is that an inversion in the band structure at Γ takes place approxi-

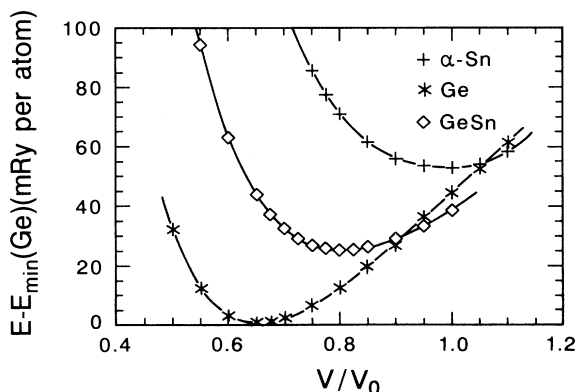


FIG. 2. Total energies (in mRy per atom) of α -Sn (+), Ge (*), and SnGe (\diamond) as obtained from the full-potential LMTO calculations. V_0 is defined to be the experimental equilibrium volume for α -Sn. The calculations use two energy panels. The Ge 3*d* as well as the Sn 4*d* states are treated as fully relaxed “band” states.

TABLE II. Theoretical (from full-potential LMTO total-energy calculations) and experimental equilibrium volumes for α -Sn, Ge, and SnGe. V_0 is the experimental equilibrium volume of α -Sn ($a_0 = 6.490$ Å).

V/V_0	α -Sn	Ge	SnGe
Theory	0.989	0.653	0.803
Expt.	1.000	0.662	

mately midway between the equilibrium lattice constant given above and a somewhat larger one corresponding to the average unit-cell volume of Ge and α -Sn. The *p-s* gap is negative in the latter case (-0.72 eV) and the band structure is therefore similar to that of α -Sn. Usually a lattice constant ($a_0 = 6.101$ Å for the zinc-blende SnGe alloy) corresponding to the average unit-cell volume is taken at the equilibrium value (Vegard’s Law), but our total-energy calculations show that this cannot be justified for SnGe, and our band-structure calculations indicate that the bands are qualitatively different in the two cases.

The LMTO band structure of SnGe at the predicted equilibrium volume is shown in Fig. 3. Since the diamond structure has inversion symmetry, all bands of Ge and α -Sn are at least twofold degenerate. In the zinc-blende structure the bands split as described in Refs. 7, 18, 25, and 26. As expected, the splittings along the low-symmetry Σ direction, [110], are quite large. The reader is directed to Figs. 4–8 in Sec. V, where the pure splittings along the [110] and [111] directions are shown. Table III displays the main energy gaps and the SO splittings of the three materials at three points of high symmetry, Γ , L , and X . The SO splitting Δ_2 at X is also due to the lack of inversion symmetry in the zinc-blende structure and does not occur in diamond-type materials. The same holds for the gap between the X_6 - X_6 lowest valence states, which is calculated to be 0.798 eV in SnGe.

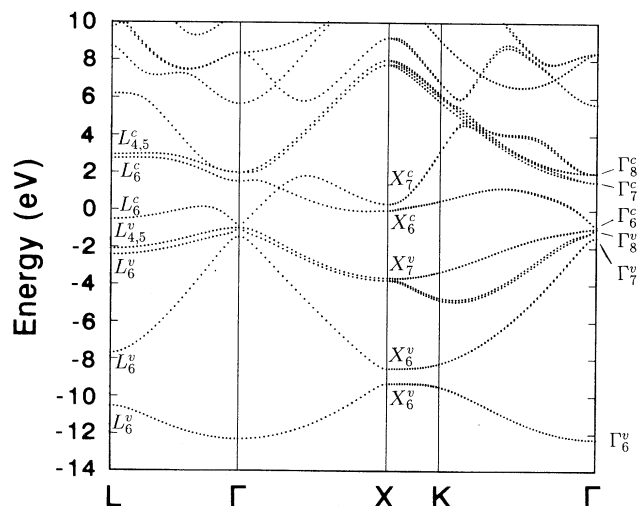


FIG. 3. Relativistic band structure of SnGe (including the correction potential) at the predicted equilibrium lattice constant of $a_0 = 6.063$ Å.

TABLE III. Calculated and experimental energy gaps and SO splittings at points of high symmetry. All energies are in eV.

	Sn		Ge		SnGe
	LMTO	Expt.	LMTO	Expt.	LMTO
E_0	-0.406	-0.413	0.868	0.89	0.0851
Δ_0	0.726	0.8	0.311	0.297	0.480
E'_0 ^a	2.055	1.98	2.932	3.01	2.504
Δ'_0	0.555	0.3-0.5	0.243	0.200	0.474
Δ^-	0	0	0	0	0.294
E_1 ^b	1.681	1.798	2.275	2.25,2.222	1.577 ^d
Δ_1	0.472	0.482	0.199	0.18 ^d	0.325 ^d
E_2 ^c	3.590	3.681	4.171	4.49	3.61
Δ_2	0	0	0	0	0.133

^a $E'_0 = E(\Gamma_6^c) - E(\Gamma_8^c)$.

^b $E_1 = E(\Lambda_6^c) - E(\Lambda_{4,5}^c)$.

^c $E_2 = E(X_5^c) - E(X_5^v)$ or $E(X_6^c) - E(X_7^v)$.

^dAt L .

III. EFFECTIVE MASSES AND MATRIX ELEMENTS

A. LMTO calculations

In order to study the finer structure around $\mathbf{k}=\mathbf{0}$, we divide the Brillouin-zone symmetry lines along the [100], [111], and [110] directions into a dense \mathbf{k} mesh. By fitting a straight line to the calculated electronic energies versus k^2 in the immediate vicinity of the point Γ , the size of the parabolic region can be checked, and the slopes yield the effective masses for the different directions. The effective masses of the s -like conduction band Γ_8 , m_c , and of the SO-split Γ_7 valence bands m_{SO} are isotropic, whereas the mass of the heavy-hole (hh) band shows strong warping. The light-hole (lh) band represents an intermediate case. The matrix element Q was calculated from Ref. 27,

$$\frac{1}{m_{hh}^{100}} = -1 + \frac{2Q^2}{E'_0 + \frac{1}{3}\Delta'_0}. \quad (2)$$

To determine P , we can use the expression²⁷

$$\frac{1}{m_{SO}} = -1 + \frac{2P^2}{3(E_0 + \Delta_0)} + \frac{4Q^2}{3(E'_0 + \frac{1}{3}\Delta'_0 + \Delta_0)}. \quad (3)$$

Because of the small p - s gap, the lowest s -conduction band has a very small mass and a pronounced non-parabolicity. Due to the $\mathbf{k}\cdot\mathbf{p}$ coupling between this band and the lh band, the latter should have a very small mass. Accordingly, the region of \mathbf{k} space around Γ where simple $\mathbf{k}\cdot\mathbf{p}$ perturbation expressions for the masses (and the spin splittings) are valid now becomes drastically reduced. This means a rather small fitting range (closer to Γ) for the $\mathbf{k}\cdot\mathbf{p}$ expressions used in the parameter extraction from the LMTO calculations. When we have to fit the expressions closer to Γ , enhanced numerical noise due to the diverging s -structure constants is also a problem.

These difficulties can be overcome, however. All our fits were carried out employing a least-squares procedure.

Within the fitting range the following equation, derived from Kane's few-band model,²⁸ should be valid:

$$\varepsilon_c(k) = \frac{1}{2}k^2 + \frac{-\bar{E}_G + \sqrt{\bar{E}_G^2 + 4KP^2k^2}}{2}, \quad (4)$$

with $\bar{E}_G = E_G - 2P'^2k^2/(E'_0 - E_0)$ and

$$K = 1 - \frac{1}{3} \left(1 + \frac{E_c + E_G - \frac{1}{2}k^2}{\Delta_0} \right)^{-1}. \quad (5)$$

E_G is the p - s gap and $\varepsilon_c(k)$ is the s -conduction-band energy referred to the bottom E_c of the band. In Kane's version, $K = \frac{2}{3}$. For a sufficiently small fitting range of \mathbf{k} it will not vary much, and since we roughly know the value of $E_G + E_c$ (taken to lie somewhere in the middle of the energy range we are fitting as seen from the band plots) it is now possible to move slightly away from the noise in the region near $\mathbf{k}=\mathbf{0}$, reevaluate K (we used the value $K = 0.726$), and from the least-squares procedure obtain a simultaneous determination of P and the p - s gap E_G . From the fit with Eq. (4) with P' determined with the tight-binding expression (see below) we obtained $P = 0.583$ and $E_G = 0.085$ eV, whereas $P = 0.588$ was found from Eq. (3). The values of the effective masses and the momentum matrix elements obtained by this procedure are listed in Table IV together with the corresponding parameters for α -Sn and Ge. Note that the experimental values of m_c and m_{SO} in the table are somewhat lower than the calculated ones.

B. Tight-binding estimate of P'

P' can be estimated with a simple tight-binding argument. It is zero by symmetry in diamond semiconductors, but nonzero for zinc-blende materials. Assuming that the Γ_{15}^v and Γ_{15}^c wave functions are obtained as bonding and antibonding linear combinations of the Ge and Sn p states, we can write

$$|\Gamma_{15}^v\rangle = \alpha|\text{Ge}\rangle + \beta|\text{Sn}\rangle, \quad |\Gamma_{15}^c\rangle = \beta|\text{Ge}\rangle - \alpha|\text{Sn}\rangle. \quad (6)$$

TABLE IV. Effective masses in units of the free-electron mass, self-consistent term energies for Sn and Ge E_p and E_s (in hartree) in the SnGe compound, and matrix elements of \mathbf{p} (in a.u.).

	Sn		Ge		SnGe
	LMTO	Expt.	LMTO	Expt.	LMTO
m_c	0.087	0.058	0.050	0.037,0.042	
m_{SO}	0.051	0.041	0.128	0.095	0.078
E_p	0.12737		0.07297		
E_s	-0.1925		-0.2623		
P	0.588		0.576	0.655	0.583
Q	0.494		0.46	0.607	0.51
P'	0	0	0	0	0.194
P'''					0.52 ^a

^aAverage of Sn and Ge values taken from Refs. 34 and 35.

If we assume the same for the s states, which we distinguish from the p states with a prime,

$$|\Gamma_1\rangle = \beta'|\text{Ge}'\rangle - \alpha'|\text{Sn}'\rangle, \quad (7)$$

we can calculate P' via Eq. (1). Defining the matrix elements

$$P_{\text{inter}} = i\langle\text{Sn}|p_x|\text{Ge}'\rangle \approx i\langle\text{Ge}|p_x|\text{Sn}'\rangle \quad (8)$$

and

$$P_{\text{intra}} = i\langle\text{Sn}|p_x|\text{Sn}'\rangle \approx i\langle\text{Ge}|p_x|\text{Ge}'\rangle \quad (9)$$

we find two limiting cases⁷ in which it is possible to obtain P' without having to say more about the magnitudes of P_{inter} and P_{intra} .

(i) The coefficient of P_{inter} is negligible,

$$\frac{P'}{P} = \frac{\alpha\alpha' + \beta\beta'}{\alpha\beta' - \alpha'\beta} = \frac{\eta\eta' + 1}{\eta - \eta'}. \quad (10)$$

(ii) The coefficient of P_{intra} is negligible,

$$\frac{P'}{P} = \frac{-\alpha\beta' - \alpha'\beta}{-\alpha\alpha' + \beta\beta'} = \frac{\eta + \eta'}{\eta\eta' - 1}. \quad (11)$$

We have defined the parameters $\eta = \alpha/\beta$ and $\eta' = \alpha'/\beta'$. Referring to Eq. (6) and Fig. 1, we point out that $|\text{Sn}\rangle$ and $|\text{Ge}\rangle$ are chosen to have the positive lobe to the right, so that the coefficients satisfy $\alpha > 0$ and $\beta < 0$. The ratio of α and β can be obtained from²⁹

$$\eta = \frac{-2H_{xx}}{E_p^{\text{Ge}} - E_p^{\text{Sn}} + [(E_p^{\text{Ge}} - E_p^{\text{Sn}})^2 + 4H_{xx}^2]^{1/2}}. \quad (12)$$

Here, E_p^{Sn} and E_p^{Ge} are the atomic term values that appear on the diagonal of the tight-binding Hamiltonian. H_{xx} , the composite overlap matrix element, is a function of the bond length d , and can be written for the zinc-blende structure as³⁰

$$H_{xx} = 1.28d^{-2}. \quad (13)$$

In the above equation we have actually used the parameters of the sp^3s^* model.³¹ We calculated η from Eq. (12) to be -1.20 using the term values of Harrison.³¹ This results in an antibonding wave function Γ_{15}^c which is more cationlike, as shown in Fig. 1. Note that Harrison's term energies are free-atom-like, not self-consistent, and not dependent upon crystal volume. When we use the self-consistent term energies extracted from the LMTO calculations³² for the SnGe compound, however, we find a somewhat different value, $\eta = -1.65$. It is possible that the large magnitude of η should be viewed as a screening effect of the Sn $4d$ electrons; they screen the Sn valence $5p$ electrons which move up and transfer a large amount of charge to the Ge valence $4p$ electrons. The difference observed here clearly emphasizes the importance of self-consistent calculations.

The ratio $\eta' = \alpha'/\beta'$ (both have the same sign) for the s states follows from an expression equivalent to Eq. (12) if we replace the respective E_p 's by E_s 's and H_{xx} by $V_{ss\sigma}$

given by³¹

$$V_{ss\sigma} = -5.28d^{-2}. \quad (14)$$

This time, however, the discrepancy between Harrison's value and the LMTO value is negligible (1.20 versus 1.19, respectively) and the Γ_1 conduction electrons reside more on the Sn side ("cationlike"). In Ref. 7, the Γ_1 conduction electrons for GeSi were found to reside more on the anion side, a situation which is not observed in III-V compounds (also not in SnGe, according to the above calculations), and seems to be unique to GeSi. From Fig. 1 [or perhaps more clearly by inserting our calculated values for η and η' into Eqs. (10) and (11)], we see that SnGe is likely to correspond to case (ii), where the effect of P_{intra} can be neglected. Thus our LMTO parameters produce $P'/P = 0.33$, which also gives us the sign of P' . We used this value to fit the spin splittings (see later sections) and found, contrary to the case of GeSi,⁷ no cause for further adjustments.

IV. ESTIMATES OF Δ^- IN SnGe

A. LMTO estimate

We define the SO coupling parameter Δ^- as¹⁸

$$\Delta^- = 3\langle(\frac{3}{2}\frac{3}{2})_v|H_{\text{SO}}|(\frac{3}{2}\frac{3}{2})_c\rangle \quad (15)$$

where $|(\frac{3}{2}\frac{3}{2})_v\rangle$ represents the eigenvector of the Γ_{15}^v eigenstates. Taking the phase convention of Fig. 1 (both eigenstates are chosen real), Δ^- is real. The magnitude of Δ^- can be determined by performing calculations for the Γ_{15}^v and Γ_{15}^c states, both with and without the inclusion of SO interaction. Δ^- is responsible for the fact that the ratio of the upshift of the Γ_8 states to the downshift of the Γ_7 states is not 1:2, the interband value from first-order perturbation theory, but deviates slightly from it. Second-order perturbation theory yields, for these shifts,

$$\delta(\frac{3}{2}) = \frac{\bar{\Delta}_0}{3} - \left(\frac{\Delta^-}{3}\right)^2 \bigg/ E_{15}^{\text{ul}}, \quad (16)$$

$$\delta(\frac{1}{2}) = -\frac{2\bar{\Delta}_0}{3} - \left(\frac{2\Delta^-}{3}\right)^2 \bigg/ E_{15}^{\text{ul}},$$

where E_{15}^{ul} represents the appropriate gap between the upper and lower Γ_{15} states. $\bar{\Delta}_0$ is the SO splitting that one would have if $\Delta^- = 0$. Inserting into Eq. (16) the values $\delta(\frac{3}{2}) = 153.6$ meV and $\delta(\frac{1}{2}) = -326.7$ meV, we find for $\bar{\Delta}_0$ and Δ^- the values listed in Table III. $\bar{\Delta}_0$ is only 9.68 meV smaller than the splitting $\delta(\frac{3}{2}) - \delta(\frac{1}{2})$.

B. Tight-binding estimate

Again, the minimum-basis tight-binding method³³ is a reliable tool, in particular, to determine the sign of Δ^- . From the SO Hamiltonian we find

$$\Delta^- = \alpha\beta[\Delta_0(\text{Sn}) - \Delta_0(\text{Ge})], \quad (17)$$

$$\Delta_0 = \alpha^2\Delta_0(\text{Sn}) + \beta^2\Delta_0(\text{Ge}), \quad (18)$$

$$\Delta'_0 = \beta^2 \Delta_0(\text{Sn}) + \alpha^2 \Delta_0(\text{Ge}). \quad (19)$$

Equations (17)–(19) give $\Delta^- = 183.8$ meV, $\Delta_0 = 0.422$ eV, and $\Delta'_0 = 0.615$ eV, a moderate deviation from the LMTO results. It must be emphasized here that the mixing in of d states has not been included in the above expressions.

V. INVERSION-ASYMMETRY SPIN SPLITTING IN SnGe

A. Cubic terms along [110]

All bands are split along the Σ direction in zinc-blende-type materials. The splitting energy can be written for small k as^{18,26}

$$\Delta E = \gamma k^3, \quad (20)$$

where we define the sign to be positive if the Σ_4 state is above the Σ_3 state.¹⁸ To denote the splittings of the Γ_6^c , Γ_8^v , Γ_7^v , Γ_8^c , and Γ_7^c bands we shall use γ with the subscripts c (s conduction), hh, lh, sh (split hole), he (heavy electron), le (light electron), and sc (split conduction). Figures 4–7 show the splittings near Γ . (See Fig. 3.) The jumps in the LMTO results in the figures are indicative of small numerical errors.

We have extracted the different γ 's from our LMTO data by fitting the energy difference ΔE of the split bands to k^3 , using a very dense k mesh close to Γ . When required by theory, we added a linear term in k whose coefficient is fitted as discussed in the Sec. IV A 1. In Table V, the extracted γ 's (in units of eV \AA^3) are listed. Also given in the table are values we calculated using expressions derived from third-order (in $\mathbf{k}\cdot\mathbf{p}$) perturbation theory from states that include exactly Δ_0 , Δ'_0 , and Δ^- . The signs of the splittings are taken to be those given by perturbation theory.

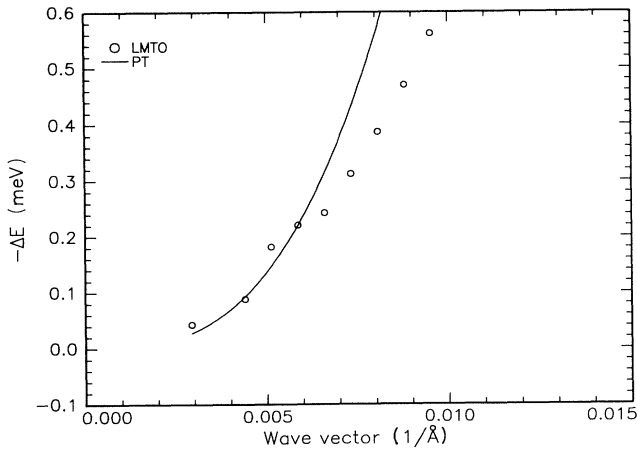


FIG. 4. Spin splitting along [110], close to Γ , of the first s -like conduction band. The LMTO results are shown as the circles. The solid curve (PT) represents the results of third-order perturbation theory. Note the effect of nonparabolicity when comparing the results of perturbation theory with those of the LMTO calculations.

1. Γ_1 band along [110]

According to fourth-order $\mathbf{k}\cdot\mathbf{p}$ perturbation theory,¹⁸ γ_c is given by

$$\gamma_c = \mathcal{A} + \mathcal{B} + \mathcal{C} + \mathcal{D}, \quad (21)$$

where

$$\begin{aligned} \mathcal{A} &= \frac{4}{3} P P' Q \frac{\Delta_0}{3E_0(E_0 + \Delta_0)} \left(\frac{2}{E'_0 - E_0 + \Delta'_0} + \frac{1}{E'_0 - E_0} \right), \\ \mathcal{B} &= \frac{4}{3} P P' Q \frac{\Delta'_0}{3(E'_0 - E_0)(E'_0 + \Delta'_0 - E_0)}, \\ \mathcal{C} &= -\frac{4}{3} \frac{P^2 Q \Delta^-}{\bar{E}_0^2 (\bar{E}'_0 - E_0)}, \\ \mathcal{D} &= -\frac{4}{3} \frac{P'^2 Q \Delta^-}{\bar{E}_0 (\bar{E}'_0 - E_0)^2}. \end{aligned} \quad (22)$$

As mentioned in earlier sections, the region where simple perturbation expressions for the splittings are valid shrinks considerably when energy gaps become small. In the Γ_1 band, the nonparabolicity starts very close to Γ and conspires with numerical noise to make an accurate parameter extraction difficult (Fig. 4). These problems lead to the failure of our numerical fitting procedure, and the extracted γ_c (Table V) is based upon geometrical fits and judgement. A similar problem occurred for the lh band. With the parameters of Table III, we calculated $\gamma_c = -272.67$ a.u. (-1104 eV \AA^3), in rather good agreement with our LMTO estimate (approximately -1094 eV \AA^3).

2. Γ_{15}^v band along [110]

The second-order $\mathbf{k}\cdot\mathbf{p}$ interaction with Γ_1 via the matrix element P (isotropic) plays an important role

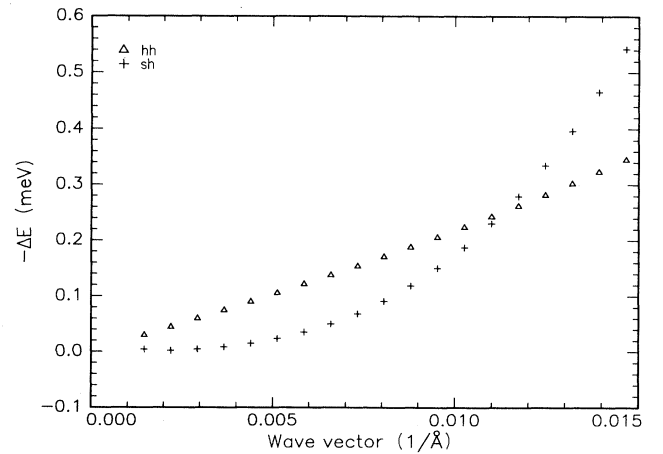


FIG. 5. Spin splitting along [110], close to Γ , of the hh band and the split-off band. The symbols denote the data for the hh and sh states as follows: Δ =hh and $+$ =sh.

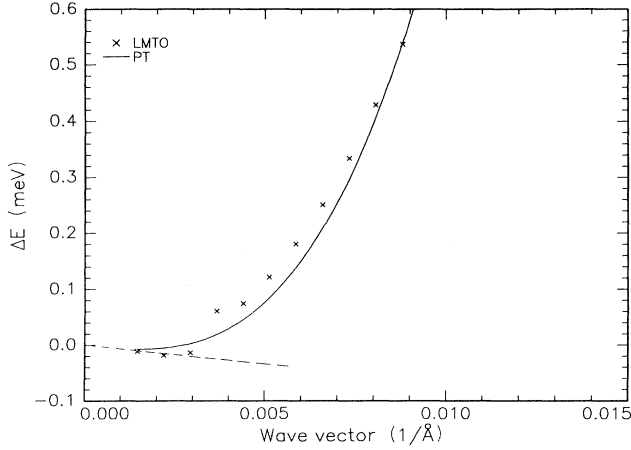


FIG. 6. Spin splitting of the lh band along [110] and close to Γ . The results of LMTO calculations are represented by the symbol \times . The solid line represents the results of perturbation theory (PT) underlying the linear and cubic k terms. The dashed line, corresponding to the linear terms, illustrates the opposite signs of the linear and cubic terms.

for these bands, and the assumption of pure angular-momentum wave functions (j, m_j) with [110] as the quantization axis can be justified. Fourth-order $\mathbf{k}\cdot\mathbf{p}$ perturbation theory predicts γ_{hh} to be zero, but a splitting due to higher-order terms can be observed in Fig. 5. The coefficient for the lh band is given by¹⁸

$$\gamma_{lh} = -\frac{4PP'Q}{3E_0\bar{E}'_0} + \frac{4P^2Q\Delta^-}{3E_0\bar{E}'_0\Delta_0} + \frac{2Q^3\Delta^-}{3E_0'^2\Delta_0}. \quad (23)$$

The lh curve is shown in Fig. 6. Extracting γ_{lh} from the LMTO calculation is difficult due to numerical noise, and the value $\sim 891 \text{ eV}\text{\AA}^3$ is the best possible estimate. We note the presence of a negative linear coefficient in the same curve. The γ_{sh} coefficient for the split-off band can be obtained from Eq. (23) by adding the corresponding SO splitting Δ_0 to the energies in the denominator, and reversing the sign. For values, see Table V.

3. Γ_{15}^c band along [110]

The Γ_7^c bands are given by $(\frac{1}{2}, \pm\frac{1}{2})$ wave functions, with [110] being the quantization axis. We take for P''' the average (0.52 a.u.) of the Sn (Ref. 34) and Ge (Ref. 35) values; 0.48 a.u. and 0.57 a.u., respectively. It is not necessary to fix the sign of this parameter, since it does not influence our calculations. According to Ref. 18,

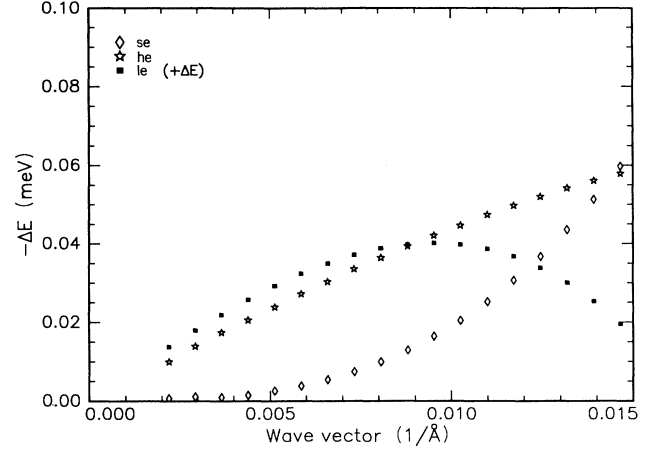


FIG. 7. Detail of the spin splitting of the lowest p -like conduction bands along [110], very close to the point Γ . The terms linear and cubic in k for the le band can easily be discerned by eye, and their relative signs determined. The symbols denote the data for the se, le, and he states as follows: \diamond =se, \blacksquare =le, and \star =he.

we have

$$\gamma_{se} = -\frac{4PP'Q}{3(E'_0 - E_0)(E'_0 + 2\Delta_0/3)} + \frac{4P'^2Q\Delta^-}{3(E'_0 - E_0)(E'_0 + 2\Delta_0/3)\Delta'_0} + \frac{2Q^3\Delta^-}{3(E'_0 + 2\Delta_0/3)^2\Delta'_0} - \frac{4P''''Q\Delta^-}{3(E''''_0 - E'_0)(E'_0 + 2\Delta_0/3)\Delta'_0}. \quad (24)$$

$$\gamma_{le} = -\frac{4PP'Q}{3(E'_0 - E_0)(E'_0 + 2\Delta_0/3)} + \frac{4P'^2Q\Delta^-}{3(E'_0 - E_0)(E'_0 + 2\Delta_0/3)\Delta'_0} + \frac{2Q^3\Delta^-}{3(E'_0 + 2\Delta_0/3)^2\Delta'_0} - \frac{4P''''Q\Delta^-}{3(E''''_0 - E'_0)(E'_0 + 2\Delta_0/3)\Delta'_0}. \quad (25)$$

Here, the fourth term is due to the interaction with the Γ_1^c band (the Γ_1 conduction band just above Γ_{15}^c).

If the Γ_8^c wave functions closely corresponded to pure angular-momentum states, γ_{le} would be obtained from Eq. (24) by adding Δ'_0 to E'_0 and reversing all signs. As can be seen from Table V, the agreement between perturbation theory and LMTO results is not bad for γ_{sc} and γ_{le} . We note especially that the huge discrepancy found for the two values of γ_{le} in GeSi (Ref. 7) does not appear in our table. For GeSi it was postulated⁷ that there was a strong mixing of the $(\frac{3}{2}, \pm\frac{3}{2})$ and $(\frac{3}{2}, \pm\frac{1}{2})$ states which gave the large value for γ_{le} and introduced a nonzero cubic coefficient $\gamma_{he} = -6.5 \text{ a.u.}$ ($-26.3 \text{ eV}\text{\AA}^3$) in the he bands. Since the discrepancy is much smaller for SnGe, and the LMTO splittings γ_{le} and γ_{sc} are close to the “experimentally adjusted” splittings of GeSi,⁷ we should

TABLE V. Values for the linear-splitting coefficients along [111] (C_k 's, in $\text{meV}\text{\AA}$) and the cubic splittings along [110] (γ 's, in $\text{eV}\text{\AA}^3$). The pure LMTO results are compared to those obtained by perturbation theory or by the semiempirical formula of Eq. (27).

	γ_c	γ_{lh}	γ_{sh}	γ_{sc}	γ_{le}	γ_{he}	C_k	C'_k
LMTO	≈ -1094	≈ 891	-173.4	-19.08	23.33	3.81	-7.72	-3.22
$\mathbf{k}\cdot\mathbf{p}$ (PT)	-1104	884.2	-125.9	-35.72	36.54		-5.91	-4.03

expect a correspondingly smaller magnitude for γ_{he} in SnGe. The value obtained, $+0.94$ a.u. (3.81 eV \AA^3), seems satisfactory. From the discussion of the linear-splitting coefficients below it will become clear that the angular momentum assumption is not particularly good for the p -like conduction bands. Also, it is likely that the value of P''' , which is very important for the cubic terms, taken from the older literature^{34,35} does not reflect the LMTO value of P''' very well.

4. Discussion

We obtain a reasonable agreement between the values of the parameters derived from our LMTO calculations and those obtained with $\mathbf{k}\cdot\mathbf{p}$ perturbation theory (Table V). The calculations are therefore consistent and support our estimates of Δ^- and P' . The LMTO results include contributions from s , p , and d levels. From the agreement between LMTO and $\mathbf{k}\cdot\mathbf{p}$ perturbation theory we conclude that the approximations made (pure J_z eigenstates, the value of Δ^- , P' , and P''' , fourth-order perturbation theory, and the number of terms included) are valid. Some caution must, however, be exercised when considering parameters pertaining to the Γ_{15}^c bands. A correct parameter extraction for these bands is difficult, due to the shortcomings of the $\mathbf{k}\cdot\mathbf{p}$ expressions available.

B. Terms linear in k

The existence of energy-level splittings linear in k in zinc-blende-type materials has been known for quite some time.^{26,36} These splittings can be measured using magneto-optical³⁷ and polariton-scattering techniques.^{38,39} We shall consider the splittings along [111] and [110] directions. For the sh, sc, and s -conduction (c) bands there are no linear terms, whereas the lh and le bands only show a linear splitting along [110]. We designate the coefficients by C_k for the valence bands and C'_k for the conduction bands.^{7,18,25}

In Ref. 18 it was demonstrated that the main contribution to C_k is the second-order interaction, bilinear in $\mathbf{k}\cdot\mathbf{p}$ and the SO operator H_{SO} between the Γ_8^v states and the uppermost d core levels (Γ_{12} intermediate states), and that the contribution from the \mathbf{k} -dependent SO Hamiltonian, which follows from first-order perturbation theory,²⁶ can be neglected. In Fig. 8 we present the splittings of the hh and he bands along [111]. The symmetries are Λ_5 and Λ_4 , respectively. For small k , the splitting along [111] is linear, and is related to the C'_k 's via^{25,26,36}

$$E(\Lambda_5) - E(\Lambda_4) = 2\sqrt{2}C_k k. \quad (26)$$

Along the [110] direction we have for the hh and lh bands, assuming pure $(\frac{3}{2} \pm \frac{3}{2})$ and $(\frac{3}{2}, \pm \frac{1}{2})$ symmetries and that we are in a region where the quadratic, effective-mass splitting dominates,^{25,26,36}

$$\begin{aligned} E(\Sigma_4) - E(\Sigma_3) &= \frac{3\sqrt{3}}{2} C_k k, \\ E(\Sigma_4) - E(\Sigma_3) &= \frac{\sqrt{3}}{2} C_k k. \end{aligned} \quad (27)$$

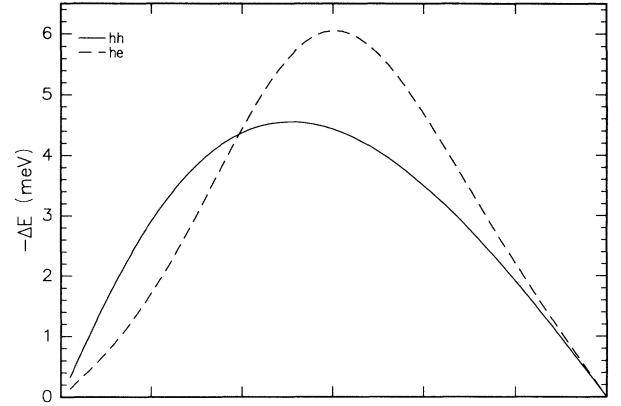


FIG. 8. Spin splittings of the hh (solid) and he (dashed) $\Gamma_8^{v,c}$ bands in SnGe for \mathbf{k} along [111] as calculated with the LMTO method.

We see from Eq. (27) a 3:1 rule for the splitting of the hh band to the splitting of the lh band along [110]. Provided that j and m_j are still good quantum numbers for he and le conduction bands, their splittings will be given by the same relationship. Since we have both cubic and linear terms present along [110] it is possible to find out by inspection in Figs. 5 and 7 the relative sign of C_k and C'_k with respect to the corresponding cubic coefficients γ . Moreover, with the signs of the γ coefficients already determined in Sec. V A, it is now straightforward to determine the absolute signs of C_k and C'_k .

The numerical fitting procedure failed for the lh splitting along [110] (Fig. 6). The linear part was therefore estimated from the splitting of the hh's, while the cubic part was determined as described in Sec. V A 2. If the approximation of pure angular-momentum states is valid, the C_k 's obtained from the splitting along [111] and along [110] using Eqs. (26) or (27) should be equal. This holds true for the hh band (7.72 meV \AA versus 7.86 meV \AA , respectively).

Fitting linear terms in the Γ_8^c bands gave the ratio 0.75/1 for the he to le linear splittings. This is comparable to the values found for III-V compounds.¹⁸ The agreement between C'_k 's obtained from the splittings of the he bands along [111] and [110] is not very good (3.22 meV \AA versus 1.83 meV \AA), indicating that the use of pure angular-momentum wave functions is not particularly appropriate for these bands. Values of C_k and C'_k (in units of meV \AA) from the fit for small k are presented in Table V.

As mentioned earlier, C_k results mainly from bilinear perturbation terms, including $H_{\mathbf{k}\cdot\mathbf{p}}$ and H_{SO} , with the Γ_{12} (core d levels) as intermediate states. In Ref. 40 the following interpolation formula was suggested:

$$C_k = -A \frac{\Delta_{d,c}}{E(\Gamma_8^v) - E_{d,c}} + B \frac{\Delta_{d,a}}{E(\Gamma_8^v) - E_{d,a}}. \quad (28)$$

Here $\Delta_{d,c}$ and $\Delta_{d,a}$ are SO splittings of the core d levels and $E_{d,c}$ and $E_{d,a}$ their energies. Taking the tabulated values from Ref. 41 and $A = B = 220 \text{ meV \AA}$, as

suggested for group-IV materials,⁴⁰ we find $C_k = -5.91$ meV Å, which is in reasonable agreement with the LMTO result (-7.72 meV Å). In Ref. 7 the corresponding GeSi calculation with $A = 220$ meV Å (Si has no core d levels) gave a result more than a factor of 2 off the LMTO value. Therefore, it was speculated⁷ that A , which is taken from the average of the cation and anion parameters for III-V and II-VI materials, may be smaller than 220 meV Å for group-IV compounds in general. Our SnGe results do not support this assumption. Alternatively, it was suggested that the lack of occupied d states in the Si cores could have unexpected effects on the splittings which could not be described by Eq. (26) with $A = 220$. In view of our SnGe calculations, the latter conclusion seems to be more reasonable, although it does not solve the quantitative problem posed by GeSi.

C'_k was found to have a negative sign. Due to the partial breakdown of the angular-momentum approximation and 3:1 rule pertaining to he and le states along [110], C'_k , as defined in Eqs. (25) and (26), will vary with direction and band. Along [111] it lies close to the corresponding GeSi value; -3.22 (SnGe) versus -3.07 meV Å (GeSi, with a p - p gap in significant error⁷). It is not immediately apparent how to relate the value for C'_k in GeSi and SnGe to those of other zinc-blende-type materials. In Ref. 18 it was suggested that only the d levels of the anion ($A \approx 0$) are important when considering the linear splittings of the Γ_{15}^c bands. If that is a general rule, we would have difficulties in explaining the sign observed here. Using Eq. (27) with $A = B = 165$ (which is the average value of A and B used for the zinc-blende materials⁴⁰), and experimental gaps and d -core SO splitting,⁴¹ the following linear coefficients are obtained: $C'_k = -4.03$ meV Å for SnGe and -2.67 meV Å for GeSi. These are in reasonable agreement with the LMTO values. With the exception of γ_{he} , the respective splitting coefficients in SnGe and GeSi have the same signs.

VI. IONICITY AND TRANSVERSE EFFECTIVE CHARGE IN SnGe

Ionicity is a somewhat qualitative concept. Harrison³⁰ has defined a polarity α_p from tight-binding parameters of the p -valence orbitals [c.f., Eq. (12)],

$$\alpha_p = \frac{E_p^c - E_p^a}{[(E_p^c - E_p^a)^2 + H_{xx}^2]^{1/2}}. \quad (29)$$

Here E_p^c and E_p^a are the term energies of cation and anion, respectively. One finds the value $\alpha_p = 0.200$ —larger than the value found for GeSi (0.07), but much smaller than the value (0.54) found for SiC,³² the only group-IV zinc-blende compound that exists in nature. According to both symmetry and the considerations discussed above, SnGe is an infrared-active material with respect to one-phonon as well as no-phonon processes; the opti-

cal phonon at Γ is associated with an electric dipole moment which can be represented by the transverse effective charge e_T^* . It is of interest to estimate e_T^* because it can give some insight into the infrared activity of phonons in Sn_n/Ge_m superlattices and also into that of the local modes in Ge and Sn. The transverse effective charge e_T^* is given by [cf. Eq. (49) of Ref. 32]

$$e_T^* = 4 \left(\alpha_p + \frac{d\alpha_p}{d \ln V} \right). \quad (30)$$

With $d\alpha_p/d \ln V = -0.834$, we obtain $e_T^* = 0.47$, a value much larger than that found for GeSi (0.09),⁷ but smaller than that of the II-VI and III-V compounds, and of SiC (~ 2.7).³² Hence the phonon-induced infrared absorption, proportional to e_T^{*2} , should be small in SnGe and in Sn_n/Ge_m superlattices for the local vibration modes of Ge in Sn.⁴²

VII. CONCLUSIONS

We have studied the band structure of zinc-blende-type SnGe using the LMTO ASA method and an empirically corrected LDA. Full-potential LMTO total-energy calculations were used to calculate the equilibrium volume, and also to investigate the stability of the SnGe compound. For technical reasons it is at present difficult to achieve sufficient accuracy in the very small total-energy differences, but preliminary results suggest, quite surprisingly, that SnGe is stable with respect to a decomposition into Ge and α -Sn. This result is tentatively supported by the recent observation of a SnGe layer in the zinc-blende structure several monolayers thick at the Sn-Ge interface in milled Sn-Ge powders.⁴³ The important band parameters for states around Γ were evaluated, the problem of parameter extraction from the highly nonparabolic s -conduction band receiving due attention. Inversion-asymmetry-induced spin splittings have been discussed, and described in terms of parametrized $\mathbf{k}\cdot\mathbf{p}$ and tight-binding perturbation theories. We point out that the k^3 terms should give rise to linear splittings in Sn_m/Ge_n superlattices, provided that both n and m are odd.⁴⁴ The ionicity and effective charge e_T^* were calculated, and the role of Sn as cation firmly established. With $e_T^* = 0.47$ there should be very weak one-phonon infrared absorption (local modes excluded) for sample thicknesses compatible with molecular-beam-epitaxy growth techniques (a few μm).

ACKNOWLEDGMENTS

The authors wish to thank M. Methfessel for the use of his full-potential LMTO code for the total-energy calculations. T.B. is indebted to the Max-Planck Gesellschaft for financial support, and O. Jepsen is thanked for a critical reading of the manuscript.

*Present address: Center for Ultrafast Optical Science, University of Michigan, 2200 Bonisteel Blvd., Ann Arbor, MI 48109-2099.

†Also at Institute of Physics, Århus University, DK-8000,

Århus C, Denmark.

¹D. W. Jenkins and J. D. Dow, Phys. Rev. B **36**, 7994 (1987).

²H. Höchst, M. A. Engelhardt, and I. Hernández-Calderón, Phys. Rev. B **40**, 9703 (1989).

- ³P. R. Pukite, A. Harwit, and S. S. Iyer, *Appl. Phys. Lett.* **54**, 2142 (1989).
- ⁴S. I. Shah, J. E. Greene, L. L. Abels, Q. Yao, and P. M. Raccach, *J. Cryst. Growth* **83**, 3 (1987).
- ⁵F. Chambouleyron and F. C. Marques, *J. Appl. Phys.* **65**, 1591 (1989).
- ⁶S. Oguz, W. Paul, T. F. Deutsch, B. Y. Tsaun, and D. V. Murphy, *Appl. Phys. Lett.* **43**, 848 (1983).
- ⁷U. Schmid, N. E. Christensen, and M. Cardona, *Phys. Rev. B* **41**, 5919 (1990).
- ⁸A. W. Ewald and O. N. Tufte, *J. Appl. Phys.* **29**, 1007 (1958).
- ⁹W. Wegscheider, K. Eberl, U. Menczigar, and G. Abstreiter, *Appl. Phys. Lett.* **57**, 875 (1990).
- ¹⁰J. Olajos, P. Vogl, W. Wegscheider, and G. Abstreiter, *Phys. Rev. Lett.* **67**, 3164 (1991).
- ¹¹J. Olajos, W. Wegscheider, and G. Abstreiter, *Appl. Phys. Lett.* **61**, 3130 (1992).
- ¹²W. Wegscheider, J. Olajos, U. Menczigar, W. Dondl, and G. Abstreiter, *J. Cryst. Growth* **123**, 75 (1992); G. Abstreiter, J. Olajos, R. Schorer, P. Vogl, and W. Wegscheider, *Semicond. Sci. Technol.* **8**, S6 (1993).
- ¹³O. K. Andersen, *Phys. Rev. B* **12**, 3060 (1975).
- ¹⁴M. Methfessel, *Phys. Rev. B* **38**, 1537 (1988).
- ¹⁵T. Brudevoll, D. S. Citrin, M. Cardona, and N. E. Christensen, *Phys. Rev. B* **48**, 8629 (1993).
- ¹⁶The actual shapes of the correcting potentials were chosen by examining the wave functions of the states that we wish to shift. The sharply peaked potentials centered on the real-atom sites mainly affect *s*-like states since only these have a finite amplitude on the nuclei. The antibonding (conduction-band minimum at Γ) are somewhat more sensitive to this than the bonding *s* states. Thus, the correcting potentials affect the unoccupied states more than the occupied states. Corrections away from $k=0$ require external potentials to be located also in the interstitial region of the zinc-blende structure. This is done by adding potentials in the "empty spheres." Earlier (see, e.g., Ref. 20) this was done by using potentials that have a form similar to those on the real atoms, but with a longer range. Since the conduction states at *L* and *X* have large amplitudes in the empty spheres, the lowest unoccupied states there can easily be tuned to experiments by varying the parameters of the potentials. In the present work (and that of Ref. 15) we decided to use a form of the potentials at the interstitial sites as given by $V_2(r)$ because this also shifts the (higher lying) conduction states.
- ¹⁷D. Munzar and N. E. Christensen (unpublished).
- ¹⁸M. Cardona, N. E. Christensen, and G. Fasol, *Phys. Rev. B* **38**, 1806 (1988).
- ¹⁹Here $|\Gamma_1\rangle$ and $|\Gamma'_1\rangle$ represent the lowest and the second lowest conduction states, respectively, of Γ_1 symmetry.
- ²⁰N. E. Christensen, *Phys. Rev. B* **30**, 5753 (1989).
- ²¹M. Alouani, S. Gopalan, M. Garringa, and N. E. Christensen, *Phys. Rev. Lett.* **61**, 1643 (1988).
- ²²I. Gorczyca, N. E. Christensen, and M. Alouani, *Phys. Rev. B* **39**, 7705 (1989).
- ²³M. S. Hybertsen and S. G. Louie, *Phys. Rev. B* **34**, 5390 (1986).
- ²⁴A. T. Paxton, M. Methfessel, and H. Polatoglou, *Phys. Rev. B* **42**, 8127 (1990).
- ²⁵M. P. Surh, M.-F. Li, and S. G. Louie, *Phys. Rev. B* **43**, 4286 (1991).
- ²⁶E. O. Kane, in *Semiconductors and Semimetals*, edited by R. K. Willardson and A. C. Beer (Academic, New York, 1966), Vol. 1.
- ²⁷M. Cardona, *J. Phys. Chem. Solids* **24**, 1543 (1963); **26**, 1351 (1965); in *Semiconductors and Semimetals* (Ref. 26), Vol. 3.
- ²⁸E. O. Kane, *J. Phys. Chem. Solids* **1**, 249 (1957).
- ²⁹A. Blacha, H. Presting, and M. Cardona, *Phys. Status Solidi B* **126**, 11 (1984).
- ³⁰W. A. Harrison, *Electronic Structure and the Properties of Solids* (Freeman, San Francisco, 1980).
- ³¹W. A. Harrison, *Phys. Rev. B* **24**, 5835 (1981).
- ³²N. E. Christensen, S. Satpathy, and Z. Pawłowska, *Phys. Rev. B* **36**, 1032 (1987).
- ³³M. Cardona, *Modulation Spectroscopy* (Academic, New York, 1969).
- ³⁴F. H. Pollak, M. Cardona, C. W. Higginbotham, F. Herman, and J. P. van Dyke, *Phys. Rev. B* **2**, 352 (1970).
- ³⁵M. Cardona and F. H. Pollak, *Phys. Rev.* **142**, 530 (1966).
- ³⁶G. Dresselhaus, *Phys. Rev.* **186**, 824 (1958).
- ³⁷C. R. Pidgeon and S. H. Groves, *Phys. Rev.* **186**, 824 (1958).
- ³⁸B. Höhnerlage, U. Rössler, V. D. Phach, A. Bivas, and J. B. Grun, *Phys. Rev. B* **22**, 797 (1980).
- ³⁹R. Sooryakumar, M. Cardona, and J. C. Merle, *Phys. Rev. B* **30**, 3261 (1984).
- ⁴⁰M. Cardona, N. E. Christensen, and G. Fasol, *Phys. Rev. Lett.* **56**, 2831 (1986).
- ⁴¹L. Ley and M. Cardona, in *Photoemission in Solids*, edited by L. Ley and M. Cardona (Springer, Heidelberg, 1979), Vol. 2, p. 377.
- ⁴²Note, however, that the infrared activity of the local modes of Si in Ge is easy to observe. See J. Humlíček, K. Navrátil, M. G. Kekoua, and E. V. Khoutsishvili, *Solid State Commun.* **76**, 243 (1990).
- ⁴³J. K. D. S. Jayanetti, S. M. Heald, and Z. Tan, *Phys. Rev. B* **47**, 2465 (1993).
- ⁴⁴S. Gopalan, M. Cardona, and N. E. Christensen, *Solid State Commun.* **66**, 471 (1988); *Phys. Rev. B* **39**, 5165 (1989).